PHYSICAL REVIEW A **77**, 031801(R) (2008)

White-light cavity with competing linear and nonlinear dispersions

Haibin Wu and Min Xiao*
Department of Physics, University of Arkansas, Fayetteville, Arkansas 72701, USA
(Received 15 October 2007; published 6 March 2008)

We experimentally demonstrate that broad, tunable bandwidth of an optical ring cavity can be achieved by making use of the negative dispersion of the Kerr nonlinear refractive index in the three-level electromagnetically-induced transparency medium. For a given cavity field intensity, the white-light cavity condition can always be satisfied by choosing the appropriate coupling beam parameters. This white-light cavity scheme can be used effectively to achieve large buildup intensity in the signal-recycling cavity with a broad bandwidth in future advanced gravitational wave detectors.

DOI: 10.1103/PhysRevA.77.031801 PACS number(s): 42.50.Gy, 42.50.Ct, 42.60.Da

Recently, several proposals and experimental demonstrations have been reported to achieve broadband cavity linewidths by using negative (anomalous) linear dispersion of intracavity media [1–4] or pair of parallel grating [5,6]. The negative dispersion can be used to compensate for the changes of the round-trip phase shifts for different frequencies and, therefore, a broad cavity bandwidth can be realized without suffering the large reduction of intensity at nearby frequencies [1]. Both of these requirements (high buildup factor for sensitivity and broad bandwidth for detecting signals at different frequencies) are essential in the next generation of gravitational wave detectors (GWD) such as GEO600 and the Advanced LIGO, when high reflectivity mirrors are used for signal recycling [7–9]. A recent experiment demonstrated a bandwidth enhancement from 5 MHz (empty cavity with intracavity elements and the cavity field tuned far off atomic resonance or 3 MHz without any intracavity elements) to about 20 MHz by placing three-level atoms inside an optical cavity with a bifrequency Raman gain [4]. The modest Raman-gain-assisted negative linear dispersion of the intracavity medium compensates for the changes of the round-trip phase shift in nearby frequencies, and broadens the cavity transmission. This technique can only apply to the cases with a relatively low buildup optical power inside the cavity since a weak probe (cavity) field is assumed in this demonstration [4]. By using two coupling beams with different frequencies, the probe field can not benefit from the two-photon Doppler-free configuration, and together with the limited Raman gain width, the achievable bandwidth in this system is limited. Higher-order dispersion, proportional to the third derivative of the linear refractive index, is a limiting factor for the achievable bandwidth in this scheme.

Here, we demonstrate an alternative mechanism to realize the white-light cavity (WLC) in the system with an intracavity electromagnetically induced transparency (EIT) [10] medium, as shown in Fig. 1. It has been well established that the Kerr nonlinear dispersion has a negative (anomalous) dispersion slope near the EIT resonance [11], which is opposite from the positive linear dispersion slope in the same frequency region [12,13], and can be quite steep comparing to the two-level atomic system. Therefore, for appropriate experimental parameters, effective index change due to the nonlinear dispersion slope at a modest given cavity intensity can be comparable or even larger than the linear dispersion slope, and the total intracavity dispersion (proportional to the group index) can take any desired signs and values including the condition for WLC [1]. Also, since the large (negative) nonlinear dispersion occurs within the EIT window and the nonlinear saturation, the impact to the cavity buildup factor can be minimized and, therefore, an effective WLC with broad transmission spectrum without sacrificing sensitivity can be achieved in this system, which can be used to improve the performance for the Advanced LIGO with signal-recycling mirrors [1–4,7–9] and other such systems for GWD. This scheme has several advantages since it can be applied to the interferometer with much higher optical powers (when nonlinearity has to be considered) and the total dispersion slope can be much fine tuned due to balancing of the linear and nonlinear dispersions with more experimen-

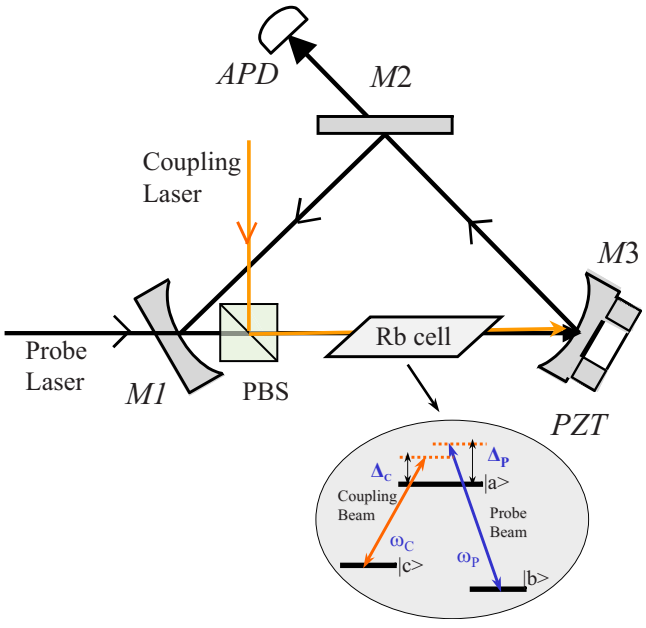

FIG. 1. (Color online) Experimental setup. PBS, polarizing cubic beam splitters; $M1-M3$, cavity mirrors; APD, avalanche photodiode detector; PZT, piezoelectric transducer. Bubble: Three-level Λ-type atomic system.

*mxiao@uark.edu

tally adjustable parameters. The achievable cavity linewidth is much broader than the ones previously demonstrated, and the mechanism to achieve such broad cavity linewidth in this work is very different from the other proposed and demonstrated mechanisms [1–6], which can stimulate other applications. For any given intracavity intensity in the current scheme, the WLC condition can always be found by adjusting other experimental parameters. Such WLC can be used not only for GWD, but also for pulse shaping, nonlinear spectroscopy, atom and ion cooling [14–16], and many other applications.

The modified cavity linewidth with an intracavity medium can be written as [17,18]

$$\Delta\nu = \frac{(\Delta\nu)_0(1-\sqrt{R_1R_2}\kappa)}{\sqrt{\kappa}(1-\sqrt{R_1R_2})}\frac{1}{1+\frac{l}{L}(n_g-1)}$$

$$= (\Delta\nu)_0'\frac{1}{1+\frac{l}{L}(n_g-1)}, \quad (1)$$

where $(\Delta\nu)_0$ is the empty cavity linewidth and $(\Delta\nu)_0'$ is the modified empty cavity linewidth with $(\Delta\nu)_0'=(\Delta\nu)_0$ for $\kappa=1$ (lossless cavity); R_1 and R_2 are the reflectivities of the input and output mirrors, respectively; $\kappa=\exp(-\alpha l/2)$ describes single-pass absorption of the medium; l and L are the lengths of the medium and the cavity, respectively. n_g is the group index of the medium, which is given by

$$n_g = (n_1+n_2I_p)+\omega_p\left[\left(\frac{\partial n_1}{\partial\omega_p}\right)+\left(\frac{\partial n_2}{\partial\omega_p}\right)I_p\right], \quad (2)$$

when the Kerr nonlinearity of the medium is taken into account. I_p is the probe (cavity) beam intensity. n_1 and n_2 are the linear and Kerr-nonlinear refractive indices, respectively. In the EIT medium, both $(\partial n_1/\partial\omega_p)$ and $(\partial n_2/\partial\omega_p)$ are greatly enhanced, and they always have opposite signs [with $(\partial n_1/\partial\omega_p)>0$ and $(\partial n_2/\partial\omega_p)<0$] within the EIT window [11,12].

When $1+(l/L)(n_g-1)=0$ in Eq. (1), the cavity linewidth becomes very broad [not infinite due to higher-order dispersion terms neglected in deriving Eq. (1)]. If the medium fills the cavity, this gives $n_g=0$. Otherwise, this condition reads

$$n_g = 1-\frac{L}{l}, \quad (3)$$

which is the so-called WLC condition [1]. Since $L>l$, $n_g<0$ is required. Near EIT resonance, both $(\partial n_1/\partial\omega_p)$ and $(\partial n_2/\partial\omega_p)$ change dramatically as functions of various parameters, such as coupling beam intensity and frequency detuning, probe beam frequency detuning, and cavity frequency detuning. Combining Eq. (3) with Eq. (2), the WLC condition can be easily satisfied by choosing appropriate parameters for a given cavity intensity I_W (which denotes the critical value at the WLC condition). The explicit expressions of linear and nonlinear refractive indices (n_1 and n_2) for a three-level Λ-type atomic system (including Doppler effect) are given in Refs. [11,12], and their derivatives over the probe frequency can be easily calculated to be used in Eq. (2). Linewidth change from below empty cavity to above empty cavity value near the condition of $n_g=1$ was previously studied in this system [19], but the possibility of achieving WLC was not realized at that time. In the present work, we concentrate on the experimental demonstration of such WLC with three-level Λ-type EIT atoms inside an optical ring cavity.

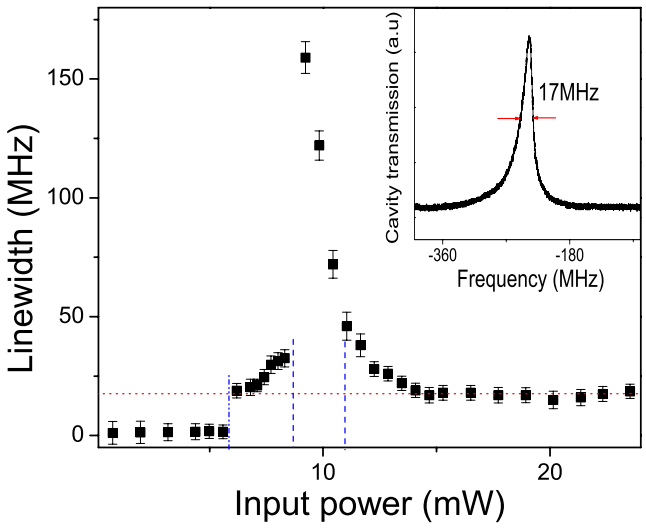

FIG. 2. (Color online) Experimentally measured cavity linewidth vs the cavity input power. Dotted horizontal line corresponds to the empty cavity linewidth; squares are the linewidths measured. Inset: "Empty" cavity transmission (at far from atomic transition). Other experimental parameters are $P_c=24$ mW coupling beam frequency detuning $\Delta_c=0$ and the cavity detuning $\Delta_\theta=-40$ MHz. $T=70$ °C.

The experiment was carried out in a system with a 5 cm long rubidium atomic vapor cell placed inside a 37 cm long ring optical cavity, as shown in Fig. 1. The transmissivities of the input and output mirrors in this three-mirror ring cavity is 3.0% and 1.4%, respectively. The third mirror is a high reflector mounted on a PZT for cavity length scanning and locking. The atomic cell has two Brewster windows and is wrapped inside μ-metal sheet for magnetic field shielding, and heated to 70 °C. Two diode lasers are used as the coupling and cavity input beams, which have linewidths of about 1.0 MHz, and are locked to reference Fabry-Pérot cavities, respectively. The coupling beam is injected through a polarization beam splitter into the cavity (not circulating in the cavity) and drives the transition between $5S_{1/2}$, $F=2-5P_{1/2}$, $F'=2$ of the ^{87}Rb. The cavity field acts as the probe field interacting with the transition $5S_{1/2}$, $F=1-5P_{1/2}$, $F'=2$. The beam waists radii are about 100 μm and 600 μm for the probe and coupling beams, respectively. The "empty" cavity finesse (with intracavity atomic cell and the polarizer, and with cavity field tuned far from atomic resonances) is about 48, corresponding to a linewidth of 17 MHz, as shown in the inset of Fig. 2. For a real empty cavity with no intracavity elements ($\kappa=1$), the linewidth is only about 5.75 MHz.

Figure 2 presents the measured cavity linewidth as a func-

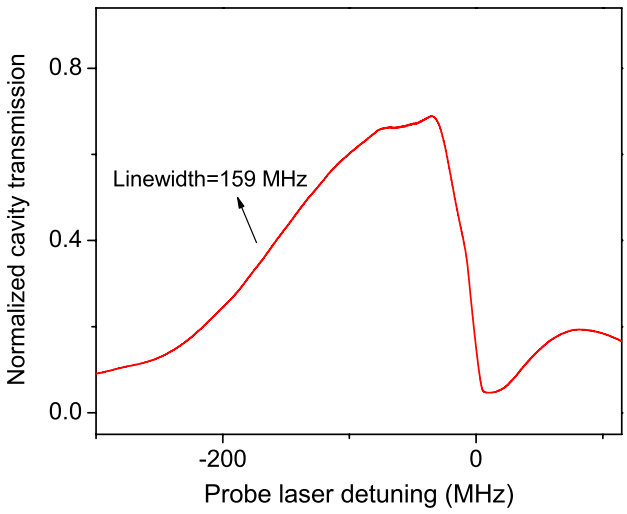

FIG. 3. (Color online) Typical cavity transmission profile when the WLC condition is satisfied. Cavity input power: 9.2 mW. Other parameters are the same as in Fig. 2.

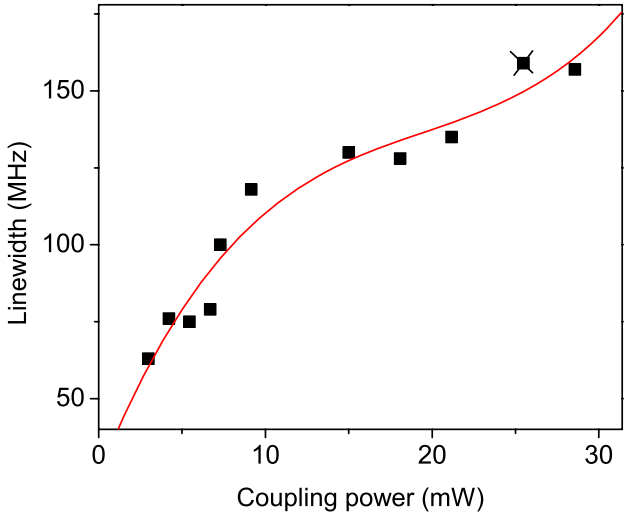

FIG. 4. (Color online) Measured cavity linewidth as a function of coupling laser power at the "critical" intensity I_W. Other experimental parameters are the same as in Fig. 2. Solid line is the best fit with a cubic function.

tion of cavity input power for a set of choosing parameters: Coupling power of 24 mW, coupling frequency detuning $\Delta_c=0$, cavity frequency detuning $\Delta_\theta=-40$ MHz, and cell temperature $T=70$ °C. The cavity transmission linewidth becomes very broad between cavity input powers of 9.0 mW and 10.5 mW, where Eq. (3) is approximately satisfied. This input power region (the input power values change slightly since a different cavity frequency detuning is used here, comparing to Ref. [19], in optimizing the broad linewidth) was not studied in Ref. [19] due to the complicated cavity transmission spectral structures. Figure 3 shows a typical cavity transmission spectrum at the cavity input power of 9.2 mW. As one can see that a quite broad cavity transmission spectrum appears with the bandwidth of about 159 MHz, which is nearly ten times broader than the "empty" cavity linewidth. It is clear that the broad cavity transmission profile is not symmetric over the probe resonance frequency, which is mainly caused by Doppler effect and nonlinearity in the cavity field. The κ value is about 0.94, corresponding to a small change in finesse due to intracavity absorption. As the input power increases from this "critical" value (corresponding to the "critical" intensity I_W, which is determined experimentally by optimizing the observable bandwidth), the sharp peak at the right of the profile becomes higher and the broad peak on the left gets suppressed, and eventually only a sharp peak at the cavity transmission survives, which approaches the empty cavity linewidth. However, as the input intensity decreases from I_W (around the input power of 9.0 mW), the broad profile starts to split in two, with the left part moving more towards left and the middle one changing slowly down to the empty cavity linewidth. The split left peak is part of the vacuum Rabi sidebands (another sideband is the broad peak at the right of the transmission profile in Fig. 3) similar to the ones observed in the two-level system [20], but modified due to the strong coupling field and the large Doppler effect at large frequency detunings. Also, the nonzero cavity detuning plays an important role in the asymmetry of the Rabi sidebands. Such complicated spectral structures are not the topic of the current work and will be investigated in detail in the future. Although the exact calculation is very hard to do since it involves nonlinearity and Doppler effect, the qualitative behaviors can be understood by considering the behaviors of the positive and negative dispersions. Although the profile of Fig. 3 is not very symmetric and flat, it nevertheless is quite broad and has high transmission (about 70% of the empty cavity transmission, similar to the result of Ref. [4]), which serves as a good demonstration of WLC.

Many parameters can be used to tune the cavity linewidth near the condition of Eq. (3). For example, if all other parameters are fixed except changing the coupling intensity, the cavity linewidth can be continuously changed, as shown in Fig. 4. As P_c is reduced, the condition of Eq. (3) will not be satisfied, and therefore the cavity bandwidth is reduced (but still much broader than the empty cavity linewidth). The point with a cross is the one satisfying Eq. (3) and can be considered as optimized. By using Eqs. (1) and (2) with the expressions of linear and nonlinear refractive indices [11,12], it can be easily shown that the cavity linewidth is a cubic function of the coupling beam power, which has been used (solid curve in Fig. 4) to fit the measured data (squares in Fig. 4).

Another very important question is whether the WLC condition can be satisfied for different intracavity intensities. Equation (3) can obviously be satisfied by many points and contours in parameter space since both linear and nonlinear refractive indices and their derivatives in Eq. (2) are sensitively dependent on various system parameters [11,12]. For a given cavity input intensity, another set of parameters can be found to reach the WLC condition [i.e., Eq. (3) can be satisfied again]. Without going through the entire parameter space, here a simple example (a cross section of the parameter space) is experimentally demonstrated. Figure 5 shows a

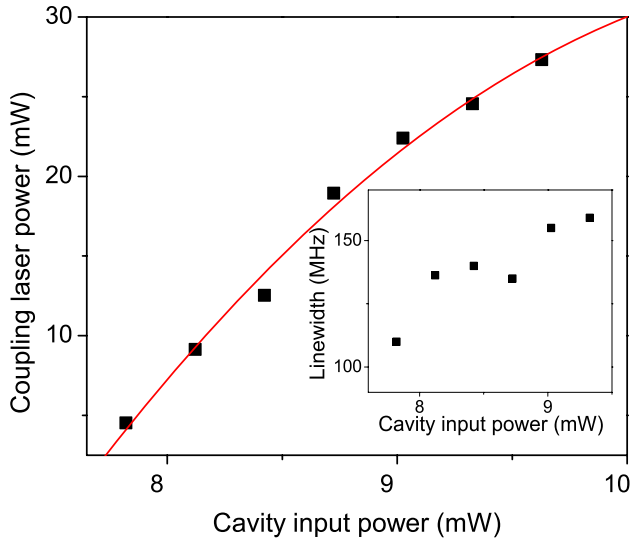

FIG. 5. (Color online) Appropriate coupling laser power for the cavity input power when the WLC condition is satisfied. Inset: The corresponding linewidths measured for each point on Fig. 5. Solid line is the best fit with a quadratic function.

contour of Eq. (3). For each cavity input intensity (power), there is a coupling beam intensity (power) to maintain the condition of Eq. (3). The corresponding linewidths measured for each point in Fig. 5 are given in the inset. One can see that for a small input power, the coupling beam intensity alone might not be able to pull the system back to satisfy the condition in Eq. (3), other parameters will need to change at the same time. The inset of Fig. 5 shows that the cavity linewidth is insensitive to the fluctuation of the input intensity which is important for certain nonlinear spectroscopic applications. Similar curves can be obtained by changing other parameters (such as cavity detuning and coupling frequency detuning). Solving Eq. (3) with explicit expressions for n_1 [12] and n_2 [11], and at near EIT resonance, the dependence of cavity input intensity over coupling power shows a quadratic relation as shown in Fig. 5 (solid curve).

Other than optimizing experimental parameters in this system to achieve an even broader cavity transmission bandwidth, a cavity with higher finesse should give more dramatic effect in enhancing the cavity linewidth. Also, this scheme of making use of the nonlinear dispersion, as well as the linear one, can be applied to EIT systems with solid materials, as well as at different wavelengths (such as 1.064 μm for the current GWD systems).

In summary, we have experimentally demonstrated a WLC by making use of the largely enhanced nonlinear dispersion in the three-level EIT system to balance the large linear dispersion, which is very different from previous works in demonstrating WLC. Broadband cavity transmission spectrum (about 159 MHz) has been achieved with certain intracavity intensity, which is important when the nonlinear effect has to be considered in the systems with signal recycling mirrors for GWDs. It is also shown that the WLC condition can be satisfied for different desired intracavity intensities by adjusting other parameters in the system, such as coupling laser power. Such broadband optical cavity can find applications in many other fields, such as pulse shaping, nonlinear optical spectroscopy, and laser cooling of atoms and ions [14–16].

We acknowledge partial funding support from the NSF (PHY-0354657 and PHY-0652970).

[1] A. Wicht, K. Danzmann, M. Fleischhauer, M. Scully, G. Muller, and R. H. Rinkleff, Opt. Commun. **134**, 431 (1997).
[2] A. Wicht, M. Muller, R. H. Rinkleff, A. Rocco, and K. Danzmann, Opt. Commun. **179**, 107 (2000).
[3] A. Rocco, A. Wicht, R. H. Rinkleff, and K. Danzmann, Phys. Rev. A **66**, 053804 (2002).
[4] G. S. Pati, M. Salit, K. Salit, and M. S. Shahriar, Phys. Rev. Lett. **99**, 133601 (2007).
[5] S. Wise, G. Mueller, D. Reitze, D. B. Tanner, and B. F. Whiting, Class. Quantum Grav. **21**, S1031 (2004).
[6] S. Wise, V. Quetschke, A. J. Deshpande, G. Mueller, D. H. Reitze, D. B. Tanner, B. F. Whiting, Y. Chen, A. Tunnermann, E. Kley, and T. Clausnitzer, Phys. Rev. Lett. **95**, 013901 (2005).
[7] B. J. Meers, Phys. Rev. D **38**, 2317 (1988).
[8] K. A. Strain and B. J. Meers, Phys. Rev. Lett. **66**, 1391 (1991).
[9] G. Heinzel, K. A. Strain, J. Mizuno, K. D. Skeldon, B. Willke, W. Winkler, R. Schilling, A. Rudiger, and K. Danzmann, Phys. Rev. Lett. **81**, 5493 (1998).
[10] S. E. Harris, Phys. Today **50**, 36 (1997).
[11] H. Wang, D. Goorskey, and M. Xiao, Phys. Rev. Lett. **87**, 073601 (2001); Opt. Lett. **27**, 258 (2002).
[12] M. Xiao, Y. Q. Li, S. Z. Jin, and J. Gea-Banacloche, Phys. Rev. Lett. **74**, 666 (1995); J. Gea-Banacloche, Y. Q. Li, S. Z. Jin, and M. Xiao, Phys. Rev. A **51**, 576 (1995).
[13] L. V. Hau, S. E. Harris, Z. Dutton, and C. H. Behroozi, Nature (London) **397**, 594 (1999).
[14] M. Zhu, C. W. Oates, and J. L. Hall, Phys. Rev. Lett. **67**, 46 (1991).
[15] A. S. Parkins and P. Zoller, Phys. Rev. A **45**, 6522 (1992).
[16] S. N. Atutov *et al.*, Phys. Rev. Lett. **80**, 2129 (1998).
[17] H. Wang, D. Goorskey, and M. Xiao, Opt. Lett. **25**, 1732 (2000).
[18] M. D. Lukin, M. Fleishhauer, M. O. Scully, and V. L. Velichaushy, Opt. Lett. **23**, 295 (1998).
[19] H. Wu and M. Xiao, Opt. Lett. **32**, 3122 (2007).
[20] J. Gripp, S. L. Mielke, L. A. Orozco, and H. J. Carmichael, Phys. Rev. A **54**, R3746 (1996).